



Since January 2020 Elsevier has created a COVID-19 resource centre with free information in English and Mandarin on the novel coronavirus COVID-19. The COVID-19 resource centre is hosted on Elsevier Connect, the company's public news and information website.

Elsevier hereby grants permission to make all its COVID-19-related research that is available on the COVID-19 resource centre - including this research content - immediately available in PubMed Central and other publicly funded repositories, such as the WHO COVID database with rights for unrestricted research re-use and analyses in any form or by any means with acknowledgement of the original source. These permissions are granted for free by Elsevier for as long as the COVID-19 resource centre remains active.



## Short communication

# Identification of a novel nidovirus associated with a neurological disease of the Australian brushtail possum (*Trichosurus vulpecula*)

M. Dunowska<sup>a,\*</sup>, P.J. Biggs<sup>a</sup>, T. Zheng<sup>b</sup>, M.R. Perrott<sup>a</sup>

<sup>a</sup>Institute of Veterinary, Animal and Biomedical Sciences, Massey University, Palmerston North, New Zealand

<sup>b</sup>AgResearch Grasslands, Hopkirk Research Institute, Palmerston North, New Zealand

## ARTICLE INFO

## Article history:

Received 12 October 2011

Received in revised form 1 November 2011

Accepted 15 November 2011

## Keywords:

Wobbly possum disease

Neurological disease

Nidovirales

Nidovirus

Arteriviridae

Arterivirus

Next generation sequencing

Emerging infections

Australian brushtail possum

## ABSTRACT

A novel, fatal neurological disease of the Australian brushtail possum (*Trichosurus vulpecula*) was first identified in 1995 in a research facility and subsequently in free-living possums in New Zealand and termed wobbly possum disease (WPD). The results of previous transmission studies suggested that the aetiological agent of WPD is most likely a virus. However, the identity of the presumed viral agent had not been elucidated. In the current report, we describe identification of a novel virus from tissues of WPD-affected possums using a combination of next generation sequencing and traditional molecular methods. The proportion of possums positive for the novel virus by PCR was significantly higher ( $p < 0.0001$ ) among animals with WPD than clinically healthy possums, strongly suggesting an aetiological involvement of the virus in WPD. Analysis of the partial genomic sequence of the putative WPD virus indicated that it is a novel nidovirus, most closely related to the current members of the family Arteriviridae.

© 2011 Elsevier B.V. All rights reserved.

## 1. Introduction

The Australian brushtail possum (*Trichosurus vulpecula*) is a marsupial native to Australia. It was introduced into New Zealand in the 19th century and has since become a significant pest to the country's ecosystem (Cowan, 2005). Very few viruses have been found among possums in New Zealand, and even fewer have been associated with clinical disease (Perrott et al., 2000b; Rice and Wilks, 1996; Thomson et al., 2002; Zheng and Chiang, 2007). A fatal neurological disease, termed wobbly possum disease (WPD), was first recognised in a research facility in 1995 (Mackintosh et al., 1995). The disease was also observed in free-living possums, and was reproduced under experimental conditions in healthy possums in contact with

diseased animals or by intra-peritoneal inoculations of filtered material prepared from spleen or liver homogenates of WPD-affected possums (O'Keefe et al., 1997; Perrott et al., 2000c). The early stages of disease are characterised by behavioural changes (loss of appetite, decreased interest in the environment, temperament changes ranging from timidity to extreme overt aggression), followed by a fine head tremor, progressive ataxia, apparent blindness and reluctance to move (Perrott et al., 2000a, 2000c). Frank blood may be detected in faeces, often in association with mucus. Almost all experimentally infected animals develop severe disease after an incubation of about two weeks. Histologically, the disease is characterised by non-suppurative meningo-encephalitis and infiltrations of mononuclear inflammatory cells, often associated with blood vessels, in several other tissues including liver or spleen (Mackintosh et al., 1995; O'Keefe et al., 1997; Perrott et al., 2000a). Currently, the presence of these histological lesions is the basis for laboratory confirmation of WPD in possums with typical clinical signs. Altogether, the results of the previous investigations

\* Corresponding author at: Institute of Veterinary, Animal and Biomedical Sciences, Massey University, Private Bag 11 222, Palmerston North 4442, New Zealand. Tel.: +64 6 3569099x7571; fax: +64 6 3505714.

E-mail address: [M.Dunowska@massey.ac.nz](mailto:M.Dunowska@massey.ac.nz) (M. Dunowska).

suggested that WPD is caused by a transmissible and filterable agent, most likely a virus. However, the identity of the presumed viral agent had not been elucidated. In the current paper, we have re-addressed the search for the aetiological agent of WPD using next generation sequencing (NGS) technology.

## 2. Materials and methods

### 2.1. Next generation sequencing

A standard inoculum (SI) that was used during earlier transmission studies (Perrott et al., 2000c) constituted the starting material for sequencing. The SI was enriched for viral nucleic acids by nuclease treatments according to principles described previously (Victoria et al., 2008). Briefly, aliquots of SI were treated with either DNase1 alone or with both DNase1 and RNase, followed by extraction of nucleic acids and cDNA synthesis. The cDNA/DNA was further amplified in a multiple displacement amplification (MDA) reaction using Illustra GenomiPhi V2 DNA amplification kit (GE Healthcare), phenol-chloroform extracted, ethanol precipitated and submitted to the Massey Genome Service for sequencing on an Illumina GAllx Genome Analyzer. Following pipe-line processing, the Illumina data were depleted of host sequences by mapping to a repeat masked version of *Monodelphis domestica* genome (the closest available to that of *T. vulpecula*) using BWA (Li and Durbin, 2009), Bowtie (Langmead et al., 2009) and SSAHA2 (Ning et al., 2001) aligners. *De novo* contigs assembled with ABySS (Simpson et al., 2009) and Velvet (Zerbino and Birney, 2008) were compared to viral sequences available in GenBank using BLAST algorithms.

### 2.2. Screening of possum tissues for arterivirus-like sequences

To further investigate the association between the novel virus and WPD, the initial arterivirus-like contig was used to design a pair of primers to amplify a 321 bp product. Each PCR reaction consisted of 0.3  $\mu$ M of each primer (WPD.A4.F: ACGTGTGTCGCGAGCTGTGG and WPD.A4.R: ACGTGGCTGGGGGTGACGAT) in 1 $\times$  PCR buffer (Fast Start master mix, Roche). Cycling conditions consisted of the initial denaturation (95 °C for 10 min), followed by 35 cycles of denaturation (95 °C for 15 s), annealing (65 °C for 15 s) and elongation (72 °C for 1 min), and the final extension (72 °C for 7 min). The PCR results were confirmed by dot blot hybridisations with the virus-specific digoxigenin labelled PCR probe (DIG probe). The PCR assay was used to screen archival tissues (spleens or filtered spleen homogenates) from WPD-affected and healthy possums for the presence of novel viral sequences. Tissues from the following possums were tested: (1) healthy possums ( $n = 18$ ) that were kept in captivity as part of an unrelated trial (Zheng and Chiang, 2007) for at least two months without showing any signs suggestive of WPD; (2) possums with histologically confirmed WPD following natural exposure ( $n = 8$ ); (3) possums with WPD following challenge ( $n = 6$ ) and control possums ( $n = 2$ ) from the 1996/97 transmission studies (Perrott et al., 2000c).

### 2.3. In situ hybridisation

Nine tissue samples from two WPD-affected and seven tissue samples from two healthy possums were tested for the presence of novel sequences by *in situ* hybridisation (ISH). The ISH was performed essentially as described by others (Liu et al., 2000), with the exception that the sections were digested with proteinase K (Roche) [20  $\mu$ g/mL] for 10–15 min at 37 °C, and hybridisations with the DIG probe diluted 1:100 in hybridisation buffer were carried overnight at 42 °C. The hybridised probe was detected using alkaline phosphate conjugated anti DIG Fab fragments (Roche) and NBT/BCIP substrate solution (Roche), and the slides were counterstained with FastRed.

### 2.4. Assembly and analysis of the partial genomic sequence of the novel virus

The partial genome of the putative WPD virus was assembled and analysed using Geneious software, including third party plugins (Drummond et al., 2010). The protein topology was assessed using TMHMM algorithms (Krogh et al., 2001). The presence of possible N-glycosylation sites was assessed using NetNGlyc 1 server (available at <http://www.cbs.dtu.dk/services/NetNGlyc/>) and the presence of N-terminal signal peptides using the SignalP 4.0 (Petersen et al., 2011). Secondary structure of RNA was predicted using pknotsRG and KnotInFrame tools (available at [http://bibiserv.techfak.uni-bielefeld.de/bibi/Tools\\_RNA\\_Studio.html](http://bibiserv.techfak.uni-bielefeld.de/bibi/Tools_RNA_Studio.html)). The NGS assembly was extended by rapid amplification of cDNA ends (RACE). Templates for RACE consisted of MDA-amplified SI prepared for NGS, unprocessed SI cDNA, or cDNA from tissues of another histologically confirmed case of WPD. The assembly was confirmed by amplification and sequencing of an overlapping set of PCR products using cDNA from the SI as a template (Fig. 1). The final assembly was then used as reference for mapping NGS data to increase the sequence depth. To further define the relationships between the virus and other nidoviruses, a phylogenetic tree was constructed based on the conserved HEL1 domain. The tree was inferred from predicted amino acid sequence alignments by a maximum likelihood method with the JTT model of amino acid substitutions using a PhyML Geneious plugin with a 1000 bootstrap value (Guindon and Gascuel, 2003).

### 2.5. Statistical analysis

Association between detection of the novel virus and clinical disease was estimated based on the analysis of a 2  $\times$  2 contingency table with  $p$  values calculated using Fisher's exact test (GraphPad InStat version 3.10 for Windows).

### 2.6. Nucleotide sequence accession number

The sequence of the novel virus was deposited in GenBank under accession number JN116253.

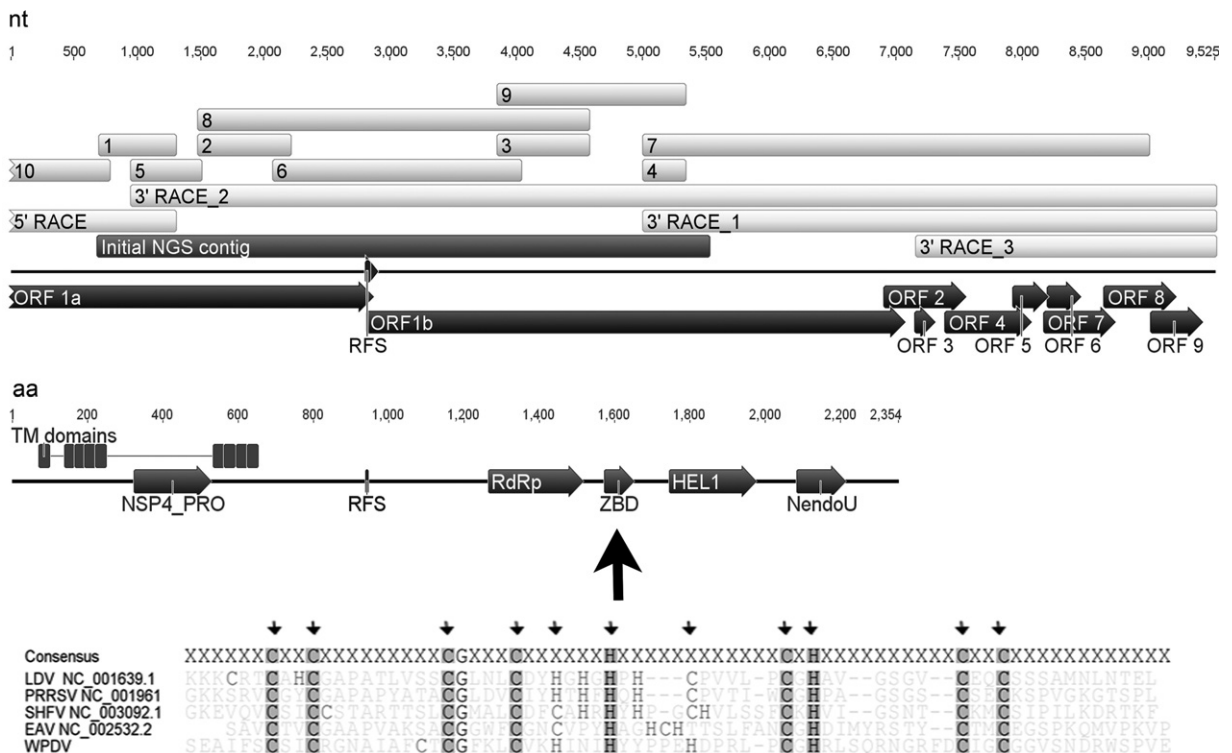


**Fig. 1.** Sequencing strategy and organisation of the partial genome of the novel nidovirus. Top: Location of predicted ORFs (boundaries as per GenBank JN116253), ribosomal frameshift site (RSF), the initial NGS contig, overlapping amplicons (1–10), and 5'/3' RACE products (primer sequences available on request). Middle: conserved protein domains including 3CL<sup>PRO</sup> (arterivirus NSP4 peptidase domain, NSP4\_PRO), transmembrane (TM), RNA-dependent RNA polymerase (RdRp), putative zinc binding domain (ZBD), viral helicase 1 (HEL1), and Nidovirus EndoU-like (NendoU) domains. Bottom: Alignment of the putative ZBD of arteriviruses (abbreviations defined in Fig. 3) with the corresponding sequence of the putative wobbly possum disease virus (WPDV). Arrows point to conserved His/Cys residues (van Dinten et al., 2000) identified in the WPDV sequence; His/Cys residues identical in all five sequences are shaded.

### 3. Results and discussion

#### 3.1. Identification of novel arterivirus-like sequences in SI and archival possum tissues

A consensus contig approximately 4.8 kb in size that returned significant TBLASTX hits to known arteriviruses was identified from the initial NGS data (Fig. 1). The viral sequence was detected in archival samples from 14/15 WPD-affected possums and from 4/20 clinically healthy possums. As such, the proportion of possums positive for the novel virus was significantly higher ( $p < 0.0001$ ) among animals with WPD than among clinically healthy possums, strongly suggesting an aetiological involvement of the virus in WPD. However, the satisfaction of more stringent criteria for establishing disease causation, including fulfilment of the original or modified Koch's postulates, is required to further support our initial findings (Williams, 2010).

#### 3.2. In situ hybridisation

Specific signal was detected in 8/9 tissues with histopathological changes characteristic of WPD (Fig. 2). The brain from one WPD-affected possum was negative for the viral sequences, although other tissues (spleen, liver,

kidney and adrenals) from that possum showed a clear virus-specific signal. The ISH signal in the brain of the second WPD-affected possum was less abundant than in other tissues tested (liver, spleen, kidney) and appeared to be associated with blood vessels adjacent to the cerebellar peduncle. This corresponds well with the distribution of histopathological lesions in WPD-affected possums reported previously (O'Keefe et al., 1997; Perrott et al., 2000a). In those studies, brain tissues from possums experimentally infected with WPD generally showed relatively mild lesions in comparison with more extensive pathology observed in other internal organs. No specific staining was observed in tissues from clinically healthy possums. As such, although only a limited number of tissues were tested, the results of ISH demonstrated the presence of the viral RNA in tissues with histological changes typical of WPD, and lack of the viral RNA in normal tissues, further strengthening the association between infection with the novel virus and WPD.

#### 3.3. Analysis of the partial genomic sequence of the novel virus

We have assembled a partial (9525 nt) genomic RNA sequence of the novel virus. We were unable to determine the entire 5' end of the viral RNA. Several attempts at 5' RACE

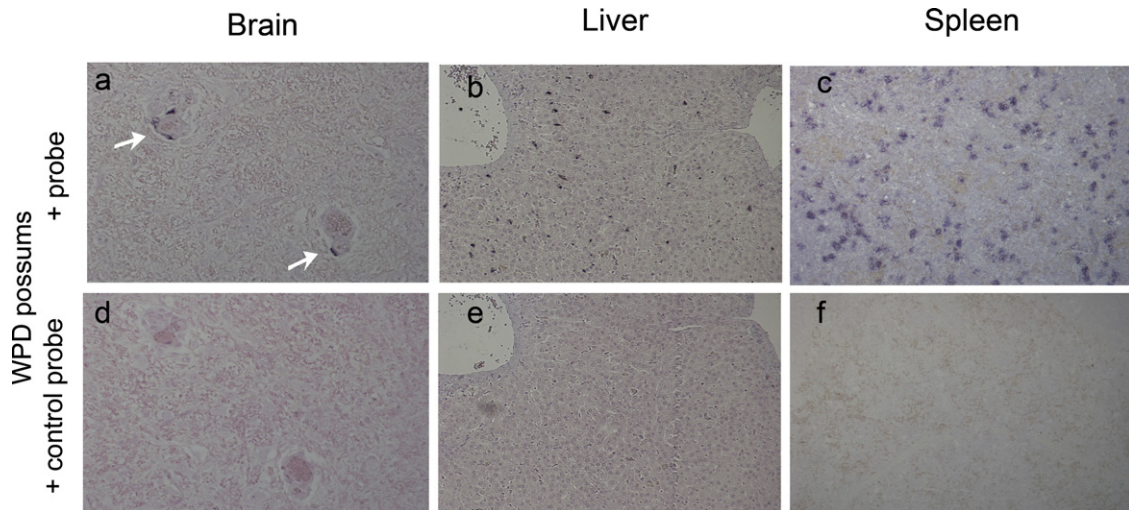


Fig. 2. An example of *in situ* hybridisation results: tissues from experimentally infected possums 674 (a and b) and 677 (c) with clinical wobbly possum disease (WPD) showing specific staining following hybridisation with the virus-specific probe (arrows in a); the same tissues hybridised with the control probe are shown in (d), (e) and (f).

yielded only one truncated PCR product from the MDA-amplified SI. The RACE product appeared to be a chimera of incorrectly joined sequences, as it could not be amplified from the original SI cDNA. This was likely the result of the use of MDA, as formation of chimera artifacts have been described as one of the important limitations of this method, particularly with relation to genome assembly from NGS data (Lasken and Stockwell, 2007; Rosario et al., 2009). Predicted coding regions consisted of 10 ORFs including (from 5' to 3') a partial sequence of *ORF1a*, the entire *ORF1b*, eight short ORFs (*ORF2–9*) predicted to code for structural proteins, a 3' untranslated region, and a polyA tail (Fig. 1). The order *Nidovirales* comprises viruses from three viral families (*Corona-*, *Arteri-* and *Roniviridae*) with diverse physicochemical and biological properties that share common genome organisation and replication strategies (Fauquet et al., 2005). All nidoviruses encode a large replicase polyprotein (pp), which is expressed from two *ORFs*: *1a* and *1b*, linked by a  $-1$  ribosomal frameshift site (RFS) (Ziebuhr et al., 2000). A slippery sequence (<sub>2820</sub>UUUAAAC<sub>2826</sub>), which has been shown to be important for ribosomal frameshifting in corona-, toro- and arteriviruses (Brierley et al., 1992), was identified in the genome of the novel virus. The viral RNA downstream from the slippery sequence (nt 2827–2881) was predicted to fold into a characteristic pseudoknot, a second element necessary for efficient ribosomal frameshifting (Kim et al., 1999). As such, it is likely that, similar to other nidoviruses, the putative WPD virus expresses *ORF1ab* through a  $-1$  RFS located in the 3' end of *ORF1a*.

All nidoviruses studied to date encode the “main” proteinase, designated 3C-like protease (3CL<sup>PRO</sup>), which is responsible for cleavage of central and C terminal portions of pp1ab to mature polypeptides (Ziebuhr et al., 2000). Analysis of the predicted pp1ab sequence of the novel virus identified the presence of the conserved GX(S/C)G catalytic motif (GD<sub>1315</sub>SG, nt 1315–1326), characteristic of chymotrypsin-like proteases, within the region homologous to the 3CL<sup>PRO</sup> of arteriviruses (non-structural protein 4). The

putative 3CL<sup>PRO</sup> (nt 979–1578) was flanked by transmembrane domains (TM) on either side, consistent with the conserved order of domains (NH<sub>2</sub>-TM1-TM2-3CL<sup>PRO</sup>-TM3-COOH) observed in other nidoviruses (Gorbalenya et al., 2006; Ziebuhr et al., 2000). With the exception of the Gill associated virus (GAV) (Cowley et al., 2000), all nidoviruses studied thus far also code for at least one additional protease located in the N terminal part of pp1a, designated papain-like protease (PLP) (Ziebuhr et al., 2000). The PLP domain was not identified within the genome of the virus, likely because we have not determined the 5' of *ORF1a*, so the region expected to code for PLP. Conserved protein domains encoded by *ORF1b* of nidoviruses include (from N- to C-terminus) RNA dependent RNA polymerase (RdRp), putative zinc-binding domain (ZBD), helicase 1 (HEL1) and uridylate-specific endoribonuclease (NendoU) domains (Gorbalenya et al., 2006). Two of these domains, ZBD and NendoU have thus far been identified only in nidoviruses and hence, have been proposed to qualify as genetic markers for the order (Ivanov et al., 2004; Nedialkova et al., 2009). We have identified RdRp (nt 3804–4541), HEL1 (nt 5247–5918) and NendoU-like (nt 6258–6632) domains in the viral genome through searches of InterProScan databases (Geneious plugin) and the Conserved Domain Database at NCBI. The relative positions of RdRp and HEL1 was characteristic for nidoviruses, as it is reversed (RdRp located downstream of HEL1) in all other positive sense RNA viruses in which both domains are present (Gorbalenya et al., 2006; Ziebuhr et al., 2000). The presence of the putative ZBD domain (nt 4718–4943) was predicted in the region containing 12 His/Cys residues, 11 of which aligned with conserved Cys/His residues in the ZBDs of other arteriviruses (van Dinten et al., 2000) (Fig. 1). Two other domains, 3'-to-5' exoribonuclease (ExoN) and ribose-2'-O-methyltransferase (O-MT), both located in the C-terminal part of the pp1ab, are conserved among large nidoviruses (corona-, toro- and roniviruses), but absent from the pp1ab of

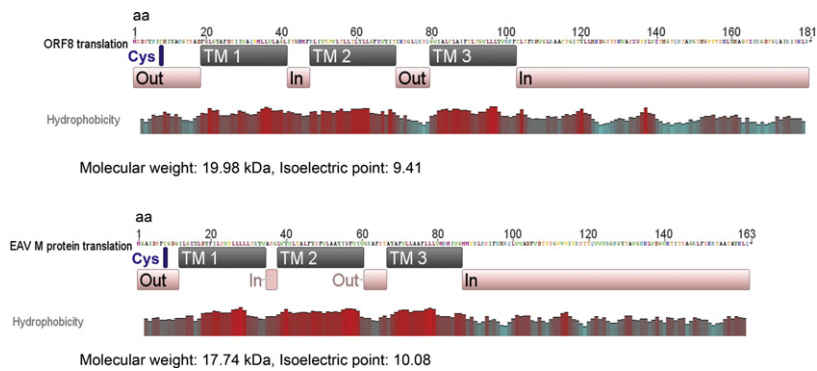


Fig. 3. Computer-based sequence analysis of the putative ORF8 protein. The same predicted features of the Equine arteritis virus (EAV, GenBank accession NC\_002532.2) protein M are shown for comparison.

arteriviruses (Gorbalenya et al., 2006). We have not identified either ExoN or O-MT domains, which further supports the closer relationship of the novel virus to arteriviruses than to any of the large nidoviruses.

The presence of several short *ORFs* downstream of *ORF1b* is consistent with the general genomic organisation of nidoviruses (Gorbalenya et al., 2006; Pasternak et al., 2006). Three major structural components of arterivirus particles include the major membrane glycoprotein (GP), main envelope (M) and nucleocapsid (N) proteins (Snijder and Spaan, 2007). A small (predicted weight of 13.4 kDa), highly basic (isoelectric point 12.21) protein with high content of Arg in the N-terminal portion (27.5% of the first 50 aa) was predicted to be encoded by *ORF9* (nt 9032–9412) of the novel virus. The position, size, and the charge of this protein suggest that it may be the equivalent of the arterivirus N protein (Snijder and Meulenberg, 1998). The putative *ORF8* (nt 8659–9201) encodes a protein of a predicted size of 20 kDa. Its size, hydrophobicity profile and the presence of three membrane spanning domains in the N-terminal part are all consistent with the structural characteristics of the M proteins encoded by arteri-, corona- and toroviruses (Gorbalenya et al., 2006; Snijder and Meulenberg, 1998) (Fig. 3). The putative short N-terminal ectodomain (aa 1–18) contains a Cys residue (aa 8), which was shown to be important for formation of the di-sulphate linked heterodimers with the major envelope GP during the life cycle of several arteriviruses (de Vries et al., 1995; Faaberg et al., 1995). Both the putative *ORF2* (nt 6917–7540) and *ORF4* (nt 7402–8055) products were predicted to comprise proteins 24 kDa in size each, with several features similar to those described for the major GP of other arteriviruses (Gorbalenya et al., 2006; Snijder and Meulenberg, 1998). These include the presence of a signal sequence (aa 1–24 or 1–25 for *ORF2* and 4, respectively), two (aa 53 and 147 for *ORF2*) or eight (aa 27, 43, 71, 76, 98, 122, 139, and 166 for *ORF4*) N-glycosylation sites, and a C-terminal TM domain (aa 176–198), suggesting that both proteins are integral membrane proteins. Of the remaining *ORFs* located in the 3' end of the genome, a small (predicted size 10 kDa) *ORF5* (nt 7938–8189) product was predicted to be N-glycosylated (aa 40), possess an N-terminal signal peptide (aa 1–24) and a C-terminal TM region (aa 56–78). The predicted *ORF7* (nt 8211–8447) product comprises a

20 kDa protein with one TM anchor located in the C-terminal part (aa 150–172) and four potential glycosylation sites (aa 11, 26, 63 and 81). However, it was not predicted to possess a signal peptide and as such, it would be unlikely to be exposed to the glycosylation machinery *in vivo*. Finally, the putative *ORF6* (nt 8186–8722) product was predicted to contain a signal sequence (aa 1–29), but no N-glycosylation sites. Taken together, similarly to other nidoviruses, the 3' region of the novel virus seems to encode several small proteins that are likely to form structural components of the virions. However, no viral or cellular homologues for these genes were identified using BLAST searches. This is consistent with the fact that structural genes of nidoviruses are highly divergent from each other, with little or no sequence homology detected between members of different families, and sometimes even between members of the same family (Gorbalenya et al., 2006; Siddell and Snijder, 2008). Hence, the true coding capacity of the 3' end of the genome needs to be corroborated based on further experimental evidence.

### 3.4. Phylogenetic analysis

The novel nidovirus clustered with other arteriviruses, although it was more distantly related to these viruses than current members of the family were to each other (Fig. 4). The patristic distances between the virus and other arteriviruses (2.145–2.197) were greater than the distances between individual arteriviruses (0.705–1.710) or individual coronaviruses (0.004–0.794), but smaller than distances between members of different families (typically between 3 and 4). However, the patristic distances between the White bream virus, which has been recently assigned to a new subfamily *Torovirinae* within the family *Coronaviridae* (Carstens, 2010), and the other members of the *Coronaviridae* family ranged from 2.8 to 3.3, so were greater than distances observed between the novel virus and arteriviruses. Similar tree topology was observed when RdRp sequences were used for alignments (data not shown). Considering the genomic features of the novel nidovirus outlined above, clustering of the virus with other arteriviruses supports its classification within the existing family *Arteriviridae*. However, relatively big genetic distances between the virus and other members of the family

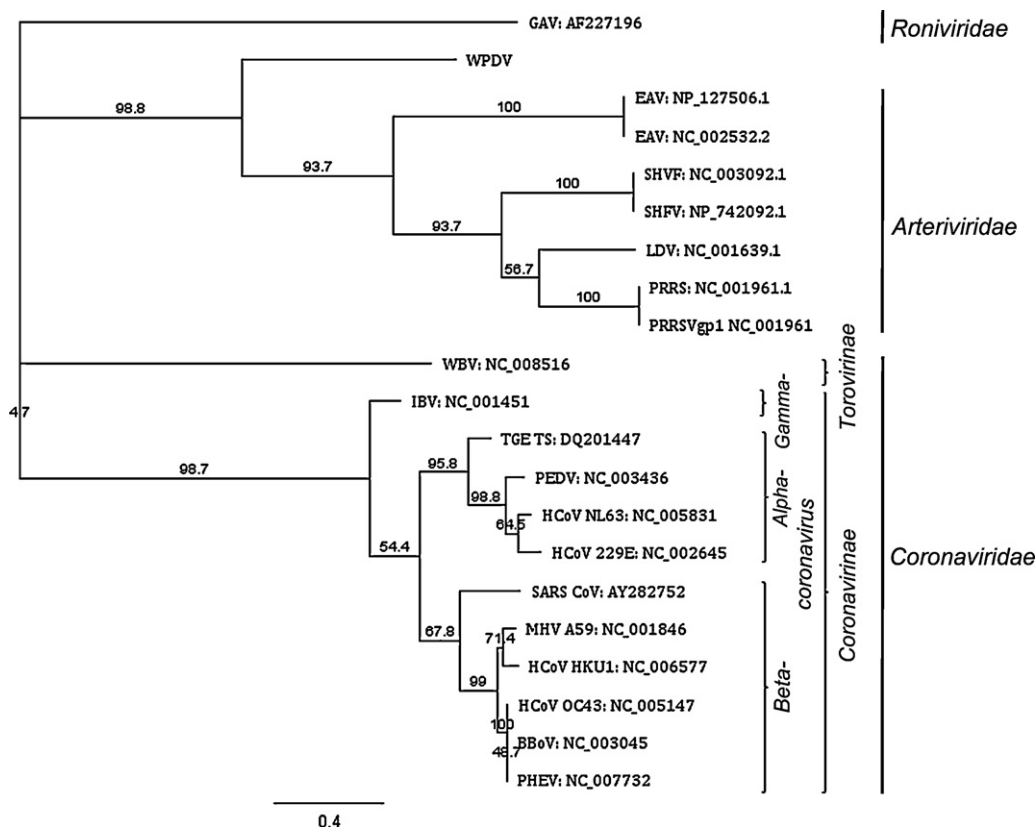


Fig. 4. Maximum likelihood phylogenetic tree inferred from predicted amino acid sequence alignments of viral helicase (HEL1) rooted using Gill associated virus (GAV) as an outgroup. The numbers at the nodes depict % of bootstrap support. Accession numbers for the sequences are listed next to the virus names. Current taxonomic classification is included on the right. Abbreviations: wobbly possum disease virus (WPDV), White bream virus (WBV), Equine arteritis virus (EAV), Simian haemorrhagic fever virus (SHFV), Lactate dehydrogenase elevating virus (LDV), Porcine respiratory and reproductive syndrome virus (PRRSV), Avian infectious bronchitis virus (IBV), Transmissible gastroenteritis virus (TGE), Porcine epidemic diarrhoea virus (PEDV), Human coronavirus (HCoV), Severe acute respiratory syndrome (SARS), Murine hepatitis virus (MHV), and Porcine hemagglutinating encephalomyelitis virus (PHEV).

may also support its placement in a new family or subfamily within the order *Nidovirales*. Further examination of the putative WPD virus, including determination of the full genomic sequence, replication strategy, and the architecture of the virion will help to decide on the most appropriate taxonomic placement for the virus.

#### 4. Conclusions

We have identified a novel virus of possums and presented initial data suggesting its aetiological involvement in WPD. Multiple lines of evidence suggest that the newly identified virus is a nidovirus. These include a nidovirus-like genome organisation, the presence and order of a conserved array of domains typical for nidoviruses and close phylogenetic relationships to the current members of the family *Arteriviridae*.

#### Acknowledgements

This work was supported by the Massey University Research Fund (RM13217), the Lewis Fitch Veterinary Research grant (RM13481), and partly by the Foundation

for Research, Science and Technology, New Zealand (C10X0501).

#### References

- Brierley, I., Jenner, A.J., Inglis, S.C., 1992. Mutational analysis of the "slippery-sequence" component of a coronavirus ribosomal frame-shifting signal. *J. Mol. Biol.* 227, 463–479.
- Carstens, E.B., 2010. Ratification vote on taxonomic proposals to the International Committee on Taxonomy of Viruses (2009). *Arch. Virol.* 155, 133–146.
- Cowan, P.E., 2005. Brushtail possum. In: King, C.M. (Ed.), *The Handbook of New Zealand Mammals*. Oxford University Press, Melbourne.
- Cowley, J.A., Dimmock, C.M., Spann, K.M., Walker, P.J., 2000. Gill-associated virus of *Penaeus monodon* prawns: an invertebrate virus with ORF1a and ORF1b genes related to arteri- and coronaviruses. *J. Gen. Virol.* 81, 1473–1484.
- de Vries, A.A., Raamsman, M.J., van Dijk, H.A., Horzinek, M.C., Rottier, P.J., 1995. The small envelope glycoprotein (GS) of equine arteritis virus folds into three distinct monomers and a disulfide-linked dimer. *J. Virol.* 69, 3441–3448.
- Drummond, A.J., Ashton, B., Buxton, S., Cheung, M., Cooper, A., Duran, C., Field, M., Heled, J., Kearse, M., Markowitz, S., Moir, R., Stones-Havas, S., Sturrock, S., Thierer, T., Wilson, A., 2010. Geneious v5.3. Available from <http://www.geneious.com>.
- Faberg, K.S., Even, C., Palmer, G.A., Plagemann, P.G., 1995. Disulfide bonds between two envelope proteins of lactate dehydrogenase-elevating virus are essential for viral infectivity. *J. Virol.* 69, 613–617.

- Fauquet, C.M., Mayo, A., Maniloff, J., Desselberger, U., Ball, L.A., 2005. Virus Taxonomy: VIIIth Report of the International Committee on Taxonomy of Viruses. Elsevier Academic Press.
- Gorbalenya, A.E., Enjuanes, L., Ziebuhr, J., Snijder, E.J., 2006. Nidovirales: evolving the largest RNA virus genome. *Virus Res.* 117, 17–37.
- Guindon, S., Gascuel, O., 2003. A simple, fast, and accurate algorithm to estimate large phylogenies by maximum likelihood. *Syst. Biol.* 52, 696–704.
- Ivanov, K.A., Hertzog, T., Rozanov, M., Bayer, S., Thiel, V., Gorbalenya, A.E., Ziebuhr, J., 2004. Major genetic marker of nidoviruses encodes a replicative endoribonuclease. *Proc. Natl. Acad. Sci. U.S.A.* 101, 12694–12699.
- Kim, Y.G., Su, L., Maas, S., O'Neill, A., Rich, A., 1999. Specific mutations in a viral RNA pseudoknot drastically change ribosomal frameshifting efficiency. *Proc. Natl. Acad. Sci. U.S.A.* 96, 14234–14239.
- Krogh, A., Larsson, B., von Heijne, G., Sonnhammer, E.L., 2001. Predicting transmembrane protein topology with a hidden Markov model: application to complete genomes. *J. Mol. Biol.* 305, 567–580.
- Langmead, B., Trapnell, C., Pop, M., Salzberg, S.L., 2009. Ultrafast and memory-efficient alignment of short DNA sequences to the human genome. *Genome Biol.* 10, R25.
- Lasken, R.S., Stockwell, T.B., 2007. Mechanism of chimera formation during the Multiple Displacement Amplification reaction. *BMC Biotechnol.* 7, 19.
- Li, H., Durbin, R., 2009. Fast and accurate short read alignment with Burrows–Wheeler transform. *Bioinformatics* 25, 1754–1760.
- Liu, X., Giambone, J.J., Hoerr, E.J., 2000. In situ hybridization, immunohistochemistry, and in situ reverse transcription-polymerase chain reaction for detection of infectious bursal disease virus. *Avian Dis.* 44, 161–169.
- Mackintosh, C.G., Crawford, J.L., Thompson, E.G., McLeod, B.J., Gill, J.M., O'Keefe, J.S., 1995. A newly discovered disease of the brushtail possum: wobbly possum syndrome. *N. Z. Vet. J.* 43, 126.
- Nedialkova, D.D., Ulferts, R., van den Born, E., Lauber, C., Gorbalenya, A.E., Ziebuhr, J., Snijder, E.J., 2009. Biochemical characterization of arterivirus nonstructural protein 11 reveals the nidovirus-wide conservation of a replicative endoribonuclease. *J. Virol.* 83, 5671–5682.
- Ning, Z., Cox, A.J., Mullikin, J.C., 2001. SSAHA: a fast search method for large DNA databases. *Genome Res.* 11, 1725–1729.
- O'Keefe, J.S., Stanislawek, W.L., Heath, D.D., 1997. Pathological studies of wobbly possum disease in New Zealand brushtail possums (*Trichosurus vulpecula*). *Vet. Rec.* 141, 226–229.
- Pasternak, A.O., Spaan, W.J., Snijder, E.J., 2006. Nidovirus transcription: how to make sense...? *J. Gen. Virol.* 87, 1403–1421.
- Perrott, M.R., Meers, J., Cooke, M.M., Wilks, C.R., 2000a. A neurological syndrome in a free-living population of possums (*Trichosurus vulpecula*). *N. Z. Vet. J.* 48, 9–15.
- Perrott, M.R., Meers, J., Greening, G.E., Farmer, S.E., Lugton, I.W., Wilks, C.R., 2000b. A new papillomavirus of possums (*Trichosurus vulpecula*) associated with typical wart-like papillomas. *Arch. Virol.* 145, 1247–1255.
- Perrott, M.R., Wilks, C.R., Meers, J., 2000c. Routes of transmission of wobbly possum disease. *N. Z. Vet. J.* 48, 3–8.
- Petersen, T.N., Brunak, S., von Heijne, G., Nielsen, H., 2011. SignalP 4.0: discriminating signal peptides from transmembrane regions. *Nat. Methods* 8, 785–786.
- Rice, M., Wilks, C.R., 1996. Virus and virus-like particles observed in the intestinal contents of the possum, *Trichosurus vulpecula*. *Arch. Virol.* 141, 945–950.
- Rosario, K., Nilsson, C., Lim, Y.W., Ruan, Y., Breitbart, M., 2009. Metagenomic analysis of viruses in reclaimed water. *Environ. Microbiol.* 11, 2806–2820.
- Siddell, S., Snijder, E.J., 2008. An introduction to Nidoviruses. In: Perlman, S., Gallagher, T., Snijder, E.J. (Eds.), *Nidoviruses*. ASM Press, Washington, DC, pp. 1–13.
- Simpson, J.T., Wong, K., Jackman, S.D., Schein, J.E., Jones, S.J., Birol, I., 2009. ABySS: a parallel assembler for short read sequence data. *Genome Res.* 19, 1117–1123.
- Snijder, E.J., Meulenbergh, J.J., 1998. The molecular biology of arteriviruses. *J. Gen. Virol.* 79 (Pt 5), 961–979.
- Snijder, E.J., Spaan, W.J.M., 2007. Arteriviruses. In: Knipe, D.M., Howley, P.M. (Eds.), *Fields Virology*. Lippincott, Williams, and Wilkins, Philadelphia, pp. 1337–1356.
- Thomson, D., Meers, J., Harrach, B., 2002. Molecular confirmation of an adenovirus in brushtail possums (*Trichosurus vulpecula*). *Virus Res.* 83, 189–195.
- van Dinten, L.C., van Tol, H., Gorbalenya, A.E., Snijder, E.J., 2000. The predicted metal-binding region of the arterivirus helicase protein is involved in subgenomic mRNA synthesis, genome replication, and virion biogenesis. *J. Virol.* 74, 5213–5223.
- Victoria, J.G., Kapoor, A., Dupuis, K., Schnurr, D.P., Delwart, E.L., 2008. Rapid identification of known and new RNA viruses from animal tissues. *PLoS Pathog.* 4, e1000163.
- Williams, J.V., 2010. Deja vu all over again: Koch's postulates and virology in the 21st century. *J. Infect. Dis.* 201, 1611–1614.
- Zerbino, D.R., Birney, E., 2008. Velvet: algorithms for de novo short read assembly using de Bruijn graphs. *Genome Res.* 18, 821–829.
- Zheng, T., Chiang, H.C., 2007. Oral challenge of brushtail possums (*Trichosurus vulpecula*) with possum enteroviruses: clinical observation, antibody response and virus excretion in faeces. *N. Z. Vet. J.* 55, 217–221.
- Ziebuhr, J., Snijder, E.J., Gorbalenya, A.E., 2000. Virus-encoded proteinases and proteolytic processing in the Nidovirales. *J. Gen. Virol.* 81, 853–879.